

The ATLAS Trigger Performance and Evolution

Brian Aagaard Petersen*

On behalf of the ATLAS Collaboration

European Laboratory for Particle Physics (CERN), Geneva

E-mail: Brian.Petersen@cern.ch

During the data taking period from 2009 until 2012, the ATLAS trigger has been very successfully used to collect proton-proton data at LHC center-of-mass energies between 900 GeV and 8 TeV. The three-level trigger system reduces the event rate from the design bunch-crossing rate of 40 MHz to an average recording rate of about 400 Hz. Using custom electronics with input from the calorimeter and muon detectors, the first level rejects most background collisions in less than 2.5 μ s. Then follow two levels of software-based triggers. The trigger system is designed to select events by identifying muons, electrons, photons, taus, jets and B hadron candidates, as well as using global event signatures, such as missing transverse energy.

We give an overview of the strategy and performance of the different trigger selections based mainly on the experience during the 2011-2012 LHC data-taking, where the trigger menu needed quick adaptations to the continuous increase of luminosity. Examples of trigger efficiencies and resolution with respect to offline reconstructed signals are presented. These results illustrate that we have achieved a very good level of understanding of both the detector and trigger performance and successfully selected suitable data samples for analysis. Furthermore, we describe how the trigger selections and overall trigger menu have been re-designed and re-optimized to cope with the increased center-of-mass energy and pileup conditions in 2012.

36th International Conference on High Energy Physics

4-11 July 2012

Melbourne, Australia

*Speaker.

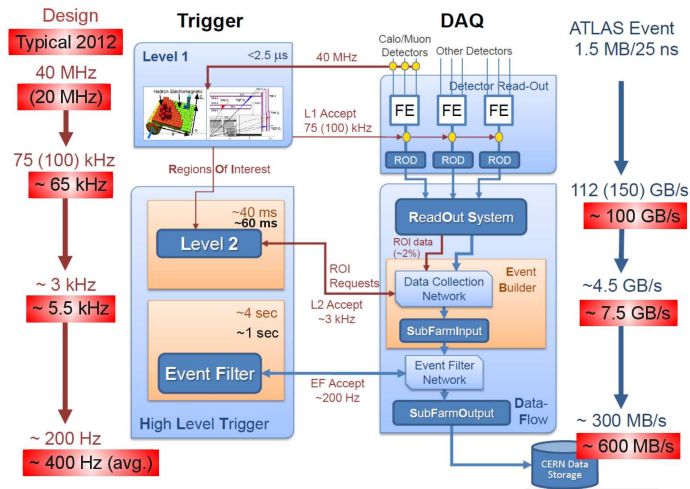


Figure 1: Overview of the ATLAS trigger and DAQ system. Both the design and typical trigger rates (left) and output bandwidth (right) for each of the three trigger levels are shown.

1. Introduction

The Large Hadron Collider (LHC) [1] is the highest energy collider in the world and has had almost three years of very successful operation with proton-proton collisions at a center-of-mass energy of 0.9–8 TeV, and with Pb-Pb collisions at 2.76 TeV per nucleon. ATLAS [2] is one of the four main experiments at the LHC and one of just two general purpose detectors designed for precision Standard Model measurements and to search for physics beyond the Standard Model. The last three years have seen a rapid increase of instantaneous (integrated) luminosity delivered by the LHC to ATLAS, from $2.0 \times 10^{32} \text{ cm}^{-1}\text{s}^{-1}$ (48 pb^{-1}) in 2010, to $3.65 \times 10^{33} \text{ cm}^{-1}\text{s}^{-1}$ (5.6 fb^{-1}) in 2011 and to $7.7 \times 10^{33} \text{ cm}^{-1}\text{s}^{-1}$ (20 fb^{-1}) in 2012. This has enabled ATLAS to set strict new limits on many new physics models and not least to discover a new Higgs-like boson [3]. At the same time the high luminosity is a challenge to the ATLAS trigger system which is responsible for selecting the few hundred most relevant collisions out of up to 500 million collisions per second. In particular the increase of the number of collisions per beam crossing (pileup) from approximately 2 in 2010, to 17 in 2011 and more than 35 in 2012, exceeding the original design value of 23 pileup events, provides a strong challenge to the trigger and necessitated multiple changes during this period. These proceedings will describe the changes to the trigger selection done to mitigate the pileup effects and the resulting performance.

2. ATLAS Trigger and DAQ System

The ATLAS trigger system [4] consists of three levels responsible for reducing the 40 MHz sampling rate (15 MHz collision rate) to between 200 and 1000 Hz of events for offline reconstruction and physics analysis with an average rate of about 400 Hz. This system is illustrated in Fig. 1. The 400 Hz limit is set by the processing power available offline for prompt event reconstruction.

The first level trigger (L1) is based on fast, custom electronics using low-granularity signals from the calorimeters and fast signals from dedicated muon trigger chambers. It requires the pres-

Signature	Peak L1 rate (Hz)	Peak L2 rate (Hz)	Average EF rate (Hz)
b-jets	5000	900	45
B-physics	7000	50	20
e/gamma	30000	2000	140
Jets	3000	1000	35
Missing E_T	4000	800	30
Muons	14000	1200	100
Tau	24000	800	35
Total	65000	5500	400

Table 1: Peak and average rates for the main trigger signatures in a typical fill in 2012 with peak instantaneous luminosity of $7 \times 10^{33} \text{ cm}^{-2}\text{s}^{-1}$. Note that there is significant overlap between the groups, particularly at L1. This is accounted for in the total.

ence of signals consistent with a hard-scattering, such as a high transverse momentum (p_T) muon, electron, jet or large missing transverse energy (E_T). It does not only reduce the rate to less than 75 kHz with a fixed latency of $2.5 \mu\text{s}$, but also defines local so-called Regions-of-Interest (RoIs) around these high- p_T objects which are used in the subsequent trigger levels.

The second (L2) and third level trigger, the latter denoted as the Event Filter (EF) and both collectively denoted as the High Level Trigger (HLT), are software-based running on large PC-farms of around 8000 cores for each level. At L2, the full event is not available. Instead, the algorithms request the data for the relevant detectors based on the RoIs defined by the L1. L2 therefore uses dedicated, fast algorithms (about 60 ms on average). In contrast, the EF has the full event data available and up to about one second for processing. The EF are based mostly on offline reconstruction algorithms adapted for the trigger in order to achieve the best performance.

The trigger selection is organized into so-called trigger chains, each consisting of one specific L1 selection seeding a sequence of selection algorithms in the HLT. Each chain is responsible for selecting a specific physics signature, such as an electron with $p_T > 25 \text{ GeV}$ or four jets with $p_T > 80 \text{ GeV}$. The full set of trigger chains is called the trigger menu and typically contains about 700 chains. It includes not only the primary physics chains (around 200), but also a large set of supporting triggers to allow measurements of backgrounds and efficiencies.

3. Trigger Menu Strategy and Evolution

The trigger menu is of critical importance for the physics program of ATLAS. If a physics signal does not have a trigger matched to its signature, it would not be possible to do the corresponding analysis or the analysis would have suboptimal sensitivity. At a given luminosity, the trigger menu is designed to have the best possible sensitivity while keeping trigger rates, CPU consumption etc. within the resource limitations of the trigger and DAQ system. At the same time the analysis preference is to have triggers with stable performance in order not to split the dataset in too many subsets. During 2011, two distinct set of menus had to be used as the peak luminosity kept rising during the year. For the first half of the year, the menu was designed for peak luminosities of $1\text{--}2 \times 10^{33} \text{ cm}^{-2}\text{s}^{-1}$, while in the later half it was optimized for $3\text{--}5 \times 10^{33} \text{ cm}^{-2}\text{s}^{-1}$.

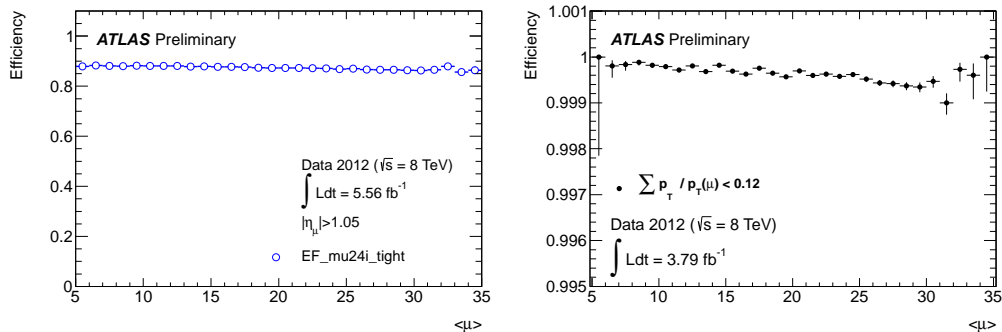


Figure 2: Efficiency of the single, isolated muon trigger (left) and of just the isolation requirement (right) versus the number of interactions per bunch crossing [5]. The efficiency is measured with respect to offline reconstructed muons in $Z \rightarrow \mu^+ \mu^-$ decays. The overall inefficiency is dominated by the L1 acceptance.

At intermediate luminosities individual triggers were disabled as needed. For 2012, the menu was redesigned to handle up to $8 \times 10^{33} \text{ cm}^{-2}\text{s}^{-1}$ and very high pileup.

In a trigger menu the bandwidth is split between different types of physics signatures depending on the importance of the signature and how refined a trigger selection is possible. The most generic triggers are the single electron and single muon triggers and these are allocated the largest bandwidth at all levels. The output rate for these is typically around 50 Hz or more each. All other multi-purpose triggers, such as multi-jets, typically have 5–15 Hz of output bandwidth, while very analysis specific triggers are constrained to around 1 Hz and therefore need quite sophisticated trigger selections. A typical distribution between different groups of physics signatures is given in Table 1. A new feature introduced in 2012 not included in the table, is the introduction of the so-called “delayed streaming”. It uses spare output capacity in the DAQ system to record an additional 150 Hz of lower p_T B-physics and jet triggers for reconstruction in 2013 when spare processing power will be available.

4. Trigger Performance

In the following the major changes to the main physics trigger signatures due to the increase in luminosity and pileup from 2011 to 2012 are summarized. Detailed descriptions of the selection algorithms for each group can be found in Ref. [4].

4.1 Muon Triggers

Triggers for muons are not affected significantly by pileup, but the increased luminosity and therefore rate, required tightening the p_T selection for most muon signatures in 2012. For the main single muon trigger, the threshold was raised from 18 to 24 GeV. In addition the muon was required to be isolated (not in a jet), by requiring the p_T sum of all tracks in a cone around the muon to be less than 12% of the muon p_T . The tracks considered in the isolation are required to have $|\Delta z| < 6\text{mm}$ in order to be pileup robust. The efficiency of the muon triggers can be measured precisely using $Z \rightarrow \mu^+ \mu^-$ decays and, as can be seen in Fig. 2, essentially no pileup dependence is seen in either the isolation requirement or the overall muon efficiency.

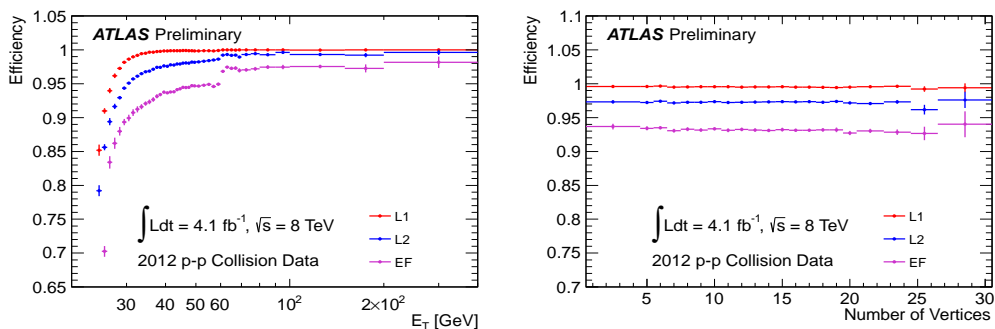


Figure 3: Efficiency of the main electron trigger as function of E_T (left) and the number of reconstructed vertices (right) [6]. The efficiency is measured with respect to offline reconstructed electrons in $Z \rightarrow e^+e^-$ decays.

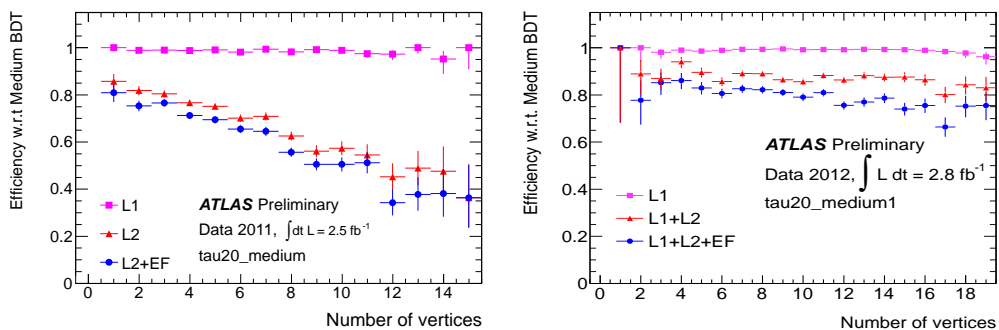


Figure 4: Cumulative trigger efficiencies at all trigger levels in 2011 (left) and 2012 (right) for a single tau selection as a function of number of reconstructed vertices [7].

4.2 Electron and Photon Triggers

The fake rate for electron triggers is significantly higher than for muons and the primary selection had to be tightened several times to keep trigger rates under control while maintaining good acceptance for electro-weak physics signals. In the middle of the 2011 run, both the L1 and HLT identification were tightened to give up to a factor two rate reduction, while for the 2012 run the selection was again retuned to remove a residual pileup dependence. Similar to the muons a track-based isolation requirement was introduced for the single electron trigger. The efficiency for the primary 2012 single electron trigger for $p_T > 25$ GeV electrons is shown in Fig. 3. No pileup dependence is seen, but the strict selection causes some loss of efficiency close to the p_T threshold.

Photon triggers use a loose, calorimeter-only selection in common with the electron triggers. The primary trigger is a di-photon trigger with thresholds optimized to provide almost 100% selection efficiency for $H \rightarrow \gamma\gamma$ events. For all of 2011, the trigger was two photons of 20 GeV, while in 2012 it was raised to 35(25) GeV for the leading(subleading) photons.

4.3 Tau Triggers

Hadronic tau decays can be identified by the presence of narrow jets with low track-multiplicity. This signal is much harder to distinguish from regular QCD jets than electrons or muons. The

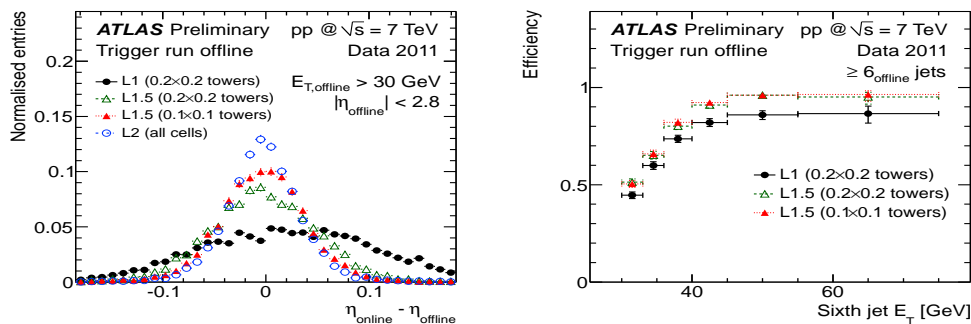


Figure 5: Left: Pseudo-rapidity resolution of different trigger jet algorithms measured with respect to offline reconstructed jets. Right: Trigger efficiency of L1 and “L1.5” 6-jet triggers versus p_T of the sixth offline reconstructed jet [9].

hadronic tau trigger is therefore mostly used in combination with other triggers such as an electron, muon or other tau triggers to select, for instance, $H \rightarrow \tau\tau$ events. Even in combined triggers, a very selective trigger is employed. It was found that the HLT selection used in 2011 had inefficiencies at large pileup as can be seen in Fig. 4. This was largely remedied for the 2012 run, by considering only the energy depositions in a smaller cone than in 2011 and by only considering tracks with a small difference in position along the beam-axis. In addition, the EF selection was switched to a multi-variate (boosted decision tree) based selection to better match the offline selection. This allowed to keep the same p_T thresholds as in 2011.

4.4 Jet Triggers

The use of RoI-based reconstruction in the jet triggers was reduced as it was found to have reduced efficiency for close-by jets. In 2011 the EF jet algorithm was changed to use clusters from the calorimeter to form jets using an anti-kt algorithm [8]. In 2012, a similar strategy has been implemented at the L2, using a full-scan algorithm over the L1 trigger towers rather than the calorimeter cells as the complete set cannot be read out at the L2 input rate. The algorithm, known as “L1.5 jets”, uses $\Delta\eta \times \Delta\phi = 0.1 \times 0.1$ trigger towers, rather than the 0.2×0.2 trigger towers used at L1. This leads to better jet resolution, as can be seen in Fig. 5. The efficiency gain for a 6-jet selection when using L1.5 jets is illustrated as well.

4.5 Missing Energy Triggers

The missing energy trigger is implemented as a vectorial sum of the energy deposited in the calorimeters. In 2011, the sum was calculated at L1 using all towers above a nominal noise threshold of about 1.2 GeV and, at EF, it was calculated using all cells above three times the expected noise level, while no calculation was done at L2. This configuration had a strong pileup dependence in the trigger rate and required a tight missing E_T threshold to be applied. In 2012, the noise thresholds in the forward ($|\eta| > 2.5$) part of the calorimeters were raised significantly (up to 10 GeV for certain L1 towers) as this is the most sensitive region to pileup. The readout electronics of the calorimeters were also upgraded to provide an energy sum of all cells in each individual readout board. These are read out and summed quickly at the L2 resulting in an improved resolution, see

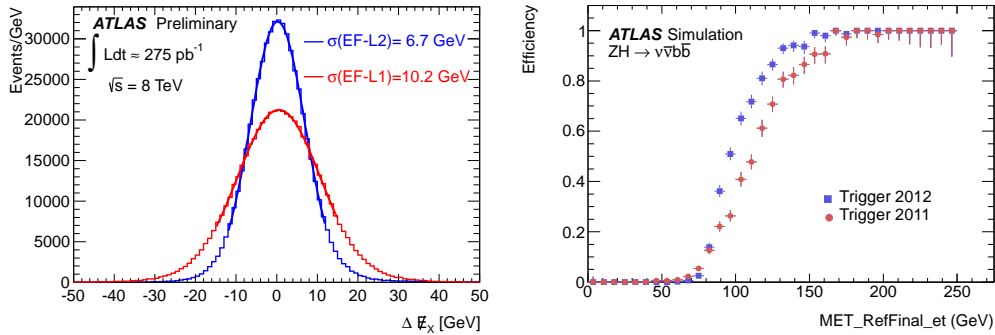


Figure 6: Left: Missing E_T resolution (for the x -component) of L1 and L2 missing E_T measured with respect to the EF missing E_T . Right: Efficiencies of the primary missing E_T triggers in 2011 and 2012 as a function of the offline reconstructed missing E_T , as measured in a simulated $ZH \rightarrow \nu\bar{\nu}b\bar{b}$ sample [10].

Fig. 6, and a rate reduction of a factor 5 or more. At the EF, the algorithm was changed to a sum over clusters calibrated to hadronic scale allowing additional pileup robustness and better resolution with respect to offline reconstructed missing energy. As can be seen in the figure, the new selection resulted in better acceptance for the missing energy trigger in 2012 than 2011, despite the luminosity and pileup being more than a factor two higher.

5. Summary

The ATLAS trigger system has operated successfully during the 2009-2012 run of the LHC. The rapidly rising luminosity and pileup conditions has been a challenge to the trigger. It needed to evolve many of its selections several times to keep both high efficiency for the most interesting physics channels and within the available bandwidth. This challenge has been met and significant improvements were deployed in time for the 2012 run.

References

- [1] L. Evans and P. Bryant, *LHC Machine*, JINST 3 (2008) S08001.
- [2] The ATLAS Collaboration, *The ATLAS Experiment at the CERN Large Hadron Collider*, JINST 3 (2008) S08003.
- [3] The ATLAS Collaboration, *Observation of a new particle in the search for the Standard Model Higgs boson with the ATLAS detector at the LHC*, Phys. Lett. B **716** (2012) 1.
- [4] The ATLAS Collaboration, *Performance of the ATLAS Trigger System in 2010*, Eur. Phys. J. C **72** (2012) 1849.
- [5] <https://twiki.cern.ch/twiki/bin/view/AtlasPublic/MuonTriggerPublicResults>
- [6] <https://twiki.cern.ch/twiki/bin/view/AtlasPublic/EgammaTriggerPublicResults>
- [7] <https://twiki.cern.ch/twiki/bin/view/AtlasPublic/TauTriggerPublicResults>
- [8] M. Cacciari, G. P. Salam and G. Soyez, *The Anti- k_t jet clustering algorithm*, JHEP **0804** (2008) 063.
- [9] <https://twiki.cern.ch/twiki/bin/view/AtlasPublic/JetTriggerPublicResults>
- [10] <https://twiki.cern.ch/twiki/bin/view/AtlasPublic/MissingEtTriggerPublicResults>